Synthesis of Hydroxyapatite through Dry Mechanochemical Method and Its Conversion to Dense Bodies: Preliminary Result

S. Adzila[1,3], I. Sopyan[2], and M. Hamdi[1]

[1] Department of Engineering Design and Manufacture, University of Malaya, Kuala Lumpur, Malaysia
[2] Department of Manufacturing and Materials Engineering, International Islamic University Malaysia, Kuala Lumpur, Malaysia
[3] Department of Materials Engineering and Design, University of Tun Hussein Onn Malaysia, Johor, Malaysia

Abstract— **Hydroxyapatite (HA) powder has been prepared through mechanochemical synthesis from a dry powder mixture of calcium hydroxide $Ca(OH)_2$ and di-ammonium hydrogen phosphate $(NH_4)_2HPO_4$. Three different rotation speeds of 170 rpm (M1), 270 rpm (M2) and 370 rpm (M3) were used in this method. The as synthesized powder analyzed by FTIR and XRD confirmed the formation of HA structure with nano crystallite size in all milling speeds. XRD results showed the wide broad peaks of HA powders narrowed and crystallinity increased (31.0-42.5%) when the milling speed was accelerated to 370 rpm. The powders were compacted using cold isostatic pressing at 200 MPa and then subjected to 1150°C, 1250°C and 1350°C sintering. The sintered compacts were mechanically tested by Vickers microhardness indentation method. Powder synthesized at 370 rpm was found to have a significant hardness, 5.3 GPa obtained after 1250°C sintering.**

Keywords— **Hydroxyapatite, Mechanochemical, Milling speed, Sintering, Vickers microhardness.**

I. Introduction

Hydroxyapatite (HA) is usually used for a number of biomedical applications in the forms of granules, blocks, as coating [1-4], as composite with polymer and ceramic [5-7], for bone augmentation and middle-ear implants [4]. HA has shown also the benefits in therapeutic antitumor vaccine [8] and was useful for drug delivery and antibiotics [9-10]. HA naturally contained in human bone as the crystals within collagen. The high strength and crack resistance or fracture toughness are necessary for the reliable work of an implant in the body [11]. Many improvements have been made earlier to overcome the limitation of HA in loading application by controlling microstructures via novel sintering technique or utilization of nano powders and by adding dopants [12-13]. Development of dense HA ceramics with superior mechanical properties is possible if the starting powder is stoichiometric with better powder properties such as crystallinity, agglomeration, and morphology. A decrease in grain size to nano scale in dense sintered materials is a desired parameter to enhance the mechanical and biological properties of HA-based bioceramic materials [14].

Various morphology, stoichiometry and level of crystallinity can be achieved depend on the technique and methods use for synthesis process. There have been several methods applied in synthesized HA nanocrystalline powder consist of co-precipitation [9], emulsion/microemulsion [15], sol-gel [16], hydrothermal [17] and mechanochemical [18]. Mechanochemical method is simple and low cost compared to other methods. The chemical processes occurring during mechanical action on solids became to be more specific and versatile. Besides, mechanochemical treatment has been recently receiving attention as an alternative route in preparing materials characterized by better biocompatibility with natural bone [18, 19]. Since then, there are several studies using a wet medium in mechanical milling have been reported [20-22] instead of milling in dry condition [18,23]. In this present study, HA powder was prepared through mechanochemical route without using any wet medium. The effect of speed will be investigated into powder properties as well as sintered dense bodies.

II. Materials and Methods

The two precursors for synthesis HA powder were commercially available calcium hydroxide $Ca(OH)_2$ (R&M Chemicals) and di-ammonium hydrogen phosphate $(NH_4)_2HPO_4$ (Systerm). The reaction of the two precursors as follows

$$5Ca(OH)_2 + 3(NH_4)_2HPO_4 \rightarrow Ca_5(PO_4)_3OH + 6NH_3 + 9H_2O \quad (1)$$

In the planetary ball mill, the precursor powders with molar ratio of 1.67 Ca/P were loaded and mixed in stainless steel vials and ball as a milling medium. Powder to ball mass ratio was 1/6 and the milling time was taken to 15 hours with three different rotation or milling speeds; 170 rpm (M1), 270 rpm (M2) and 370 rpm (M3).

To determine the weight loss, the as synthesized powders were subjected to thermal analysis in a heating rate of 10°C/min from room temperature to 1300°C under atmosphere using Perkin Elmer Phyris Diamond TG-DTA equipment.

N.A. Abu Osman et al. (Eds.): BIOMED 2011, IFMBE Proceedings 35, pp. 97–101, 2011.
www.springerlink.com

Phases in the as synthesized powders were identified using an X-ray diffractometer (CuKα, Shimadzu XRD 6000 diffractometer). All measurement were performed at room temperature with the range of 2θ=25-55°C at 2°C/min scan speed. All samples were analyzed by referring to standards of the Joint Committee of Powder Diffraction Standards (JCPDS) card number, 09-0432 [24].

The functional group of both the as synthesized powders and the powders after sintering were analyzed using a Perkin-Elmer Spectrum FTIR spectrometer of 4000-400cm^{-1} scanning range with resolution of 4 cm^{-1}.

The as synthesized powders were uniaxially pressed into pellets in a steel die of 10.5 mm in diameter using 2.5 MPa loading for two minutes , followed by cold isostatic pressing (CIP) at 200 MPa for five minutes. The green bodies were sintered at three different temperatures; 1150°C, 1250°C and 1350°C with both heating and cooling rates were 5°C/min in two hours holding time. Sintered compacted powders were then subjected to Vickers microhardness testing using indentation technique (MVK H2) after polished at 1000 grid of silicon carbide.

III. Results

A. X-Ray Diffraction (XRD) Analysis

Figure 1 shows the XRD patterns of the as synthesized powder at three different milling speeds. HA characteristic with the broad peaks already appeared in lower milling speed of 170 rpm. However, the powder still containing the unreacted precursor belongs to di-ammonium hydrogen phosphate (DAP). As the milling speed increased to 270 rpm, the HA peaks intensely growth with peaks improved. The DAP peaks were not detected. At 370 rpm, the narrow peaks observed with the new peaks of HA detected at (112) and (212) compared to previous milling speeds.

The crystallite size of the powders was calculated using Scherrer formula [25]

$$D = \frac{K\lambda}{\cos\theta\sqrt{\omega^2+\omega o^2}} \quad (1)$$

where D is the crystallite size (nm); k is the shape coefficient, 0.9; λ is the wave length (nm); θ is the diffraction angle (°); ω is the experimental full width at half maximum (FWHM); ωo is the standard FHWM value. For this purpose, FWHM at (002) (2θ=25.8°) has been chosen to calculate the crystallite size. Table 1 shows the crystallite sizes of the samples. The crystallite size was not proportional with the milling speed, so it was not affected by the various speed applied. In contrast, the crystallinity of the powders was increased as the speed level up to until 370 rpm.

Table 1 Crystallite size and crystallinity of HA powder

Sample	Milling Speed (rpm)	Crystallite size (nm)	Crystallinity (%)
M1	170	4.71	31.0
M2	270	3.08	32.0
M3	370	4.87	42.5

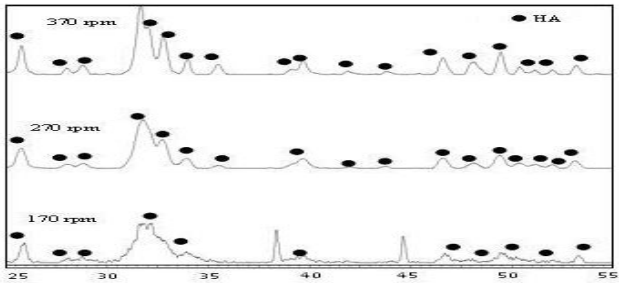

Fig. 1 XRD patterns of as-synthesized HA powder with various milling speeds

B. Thermal Gravimetric Analysis (TGA)

The graph in figure 2 shows that all of powder samples start to loss the weight below 100°C. This situation is attributed to the evaporation of adsorbed water and phase transformation occurs until 900°C. This trend was continuous until 1300°C.

C. Fourier Transform Infra Red (FTIR)

The chemical functional group of the synthesized calcium phosphate powder was determined by using FTIR analysis. Figure 3 for example shows the FTIR spectra for HA powder through dry mechanochemical synthesis with different speeds.

Phosphate (PO_4) band have four vibration modes ν1, ν2, ν3, and ν4. All samples indicate that at ν1 and ν2 modes, PO_4 band was appeared at around 962 cm^{-1} and 474 cm^{-1} respectively. ν3 mode also consist of PO_4 band at around 1088 cm^{-1} and 1023 cm^{-1}. Besides that the PO_4 band also was detected at ν4 mode at around 599 cm^{-1} and 560 cm^{-1}.

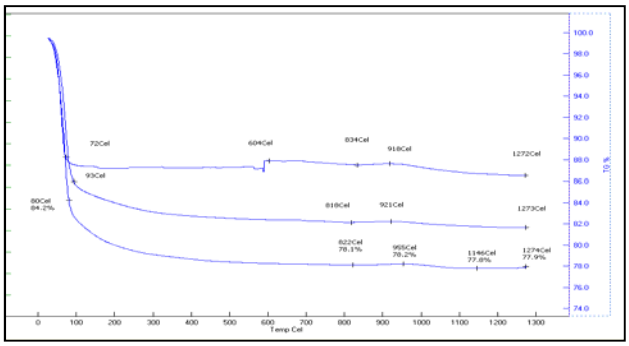

Fig. 2 TGA graphs of milled HA powders at different speed heated to 1300°C in air (heating rate=10°C/min)

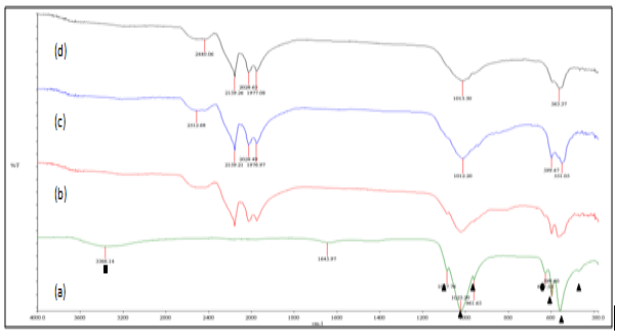

Fig. 3 The FTIR spectra of HA powder milled at 370 rpm rpm before (a) and after sintering at 1150°C (b), 1250°C (c) and 1350°C (d). [(■): H2O), (▲): PO4, (●): OH]

From M1 HA powders, ν1, ν3 and ν4 modes became weak when sintering temperature increased from 1150°C to 1350°C except for ν2 mode which disappeared when sintering temperature increased. This trend also similar with M2 and M3 HA powders.

The weak band of hydroxyl group was detected at 628 cm^{-1} [22, 26] from all of the as synthesized HA powders at different milling speeds. In M1 HA powders, the hydroxyl band exists clearly at 1150°C compared to the as synthesized powder, and changed to a weak band at 1250°C until vanished at 1350°C sintering temperature. On the other hand, M2 HA powder reduced the OH band from 1150°C to 1250°C and lost consequently at 1350°C. In contrary, the small hydroxyl band only stayed at 1150°C and fully removed at 1250°C and 1350°C.

Band around 1635-1646 cm^{-1} was attributed to the present of water in all powder samples. At the same time, the broad band of absorbed moisture can be seen at the range of 3200-3600 cm^{-1}[27]. These bands totally disappeared when subjected to the heat treatment from 1150°C to 1350°C sintering temperature.

D. Vickers Micro Hardness

The effect of sintering temperature on the Vickers hardness is shown in figure 4. In this test, M3 compacted powder yielded significant hardness, 5.3 GPa when sintered at 1250 °C followed by M1 compacted powder, 5.1 GPa sintered at 1350°C. Only hardness in M1 compacted powder was continuously increased with sintering temperature compared to M2 and M3 compacted powders which were increased initially at 1250°C and then dropped when they reached at 1350°C sintering temperature. At 1150°C, hardness in M2 compacted powder (4.6 GPa) was found higher than M3 and M1 (2.9 GPa and 2.1 GPa).

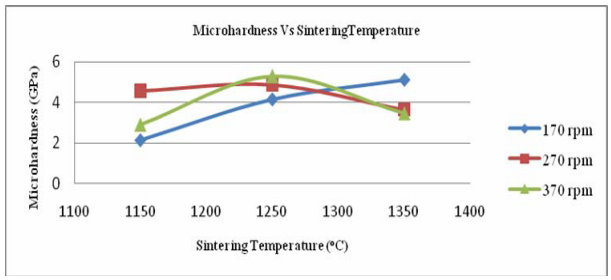

Fig. 4 Microhardness graph for sintered compacted powder samples at three different milling speed

IV. Discussion

From XRD analysis, nanocrystallite size of HA powder obtained after milling at different speed denoted as M1, M2 and M3. HA structure starts to form in early of milling speed, 170 rpm. At this speed, another phase which is believed belongs to precursor, was existed and it indicated that the process was not reacted at all. Higher milling speed has led to the formation of single HA without formation of any secondary phase. The crystallinity was increased from 31-42.5% with the milling speed and it can be seen from the peaks which were intensely growth as the speed increased. Mechanical milling on powders size did not affected by milling speed and the size around 3 to 5 nm yielded through this method. This size was significantly lower than previous study by Silva et al [28] using $CaHPO_4$, $CaCO_3$ and $NH_4H_2PO_4$ as precursors in dry milling at 370 rpm for 15 hours.

It is noted that the weight of all powder samples dropped at the range of 900°C an above might be associated with the formation of β-TCP by releasing the hydroxyl group. This condition was similar with FTIR spectra where hydroxyl

group merely disappeared as heated from 1150°C -1350°C. In addition, the phosphate band was maintained but the peak was reduced until 1350°C. During sintering process, some of impurities were detected from the band in the range of 1970 cm^{-1} - 2600 cm^{-1}. At 1150°C, greater hardness is shown by M2 compacted powder, 4.6 GPa which related to the smaller crystallite size obtained compared to M1 and M3 compacted powders. At 1250°C, significant hardness was found in M3 compacted powder, 5.3 GPa followed by M2 compacted powder. This consolidation might be attributed to the sintering effect on M3 powder compaction.

V. Conclusion

The dry mixture of $Ca(OH)_2$ and $(NH_4)_2HPO_4$ from different milling speeds has been successfully produced nanocrystalline hydroxyapatite. The milled HA at different speeds were analyzed by XRD, FTIR and TGA analysis. HA powder was obtained in all milling speeds. All of HA powders showed the continuous weight loss until 1300°C. The M3 compacted HA powder was found to have a greater hardness, 5.3 GPa at 1250°C. FTIR analysis of sintered compacted powder results in weak bands when temperature increased. The higher milling speed has increased the percent of crystallinity of the powders obtained. The morphology analysis and powder characterization after synthesized and sintering process will be carried out in future study.

Acknowledgement

The authors are grateful to Biomedical Engineering Research Group of International Islamic University Malaysia (IIUM) for supporting this research.

References

[1] M. Wei, et al. (2005) Precipitation of hydroxyapatite nanoparticles: effects of precipitation method on electrophoretic deposition," Journal of materials science. Materials in medicine, 16:319-324.

[2] S. W. K. Kweh, et al. (2000) Plasma-sprayed hydroxyapatite (HA) coatings with flame-spheroidized feedstock: microstructure and mechanical properties. Biomaterials 2: pp. 1223-1234.

[3] X. Zheng, et al.(2000) Bond strength of plasma-sprayed hydroxyapatite/Ti composite coatings. Biomaterials 21:841-849.

[4] N. Patel, et al. (2001). Calcining influence on the powder properties of hydroxyapatite. Journal of materials science. Materials in medicine 12:181-188.

[5] H. Liu and T. J. Webster (2010) Mechanical properties of dispersed ceramic nanoparticles in polymer composites for orthopedic applications. International journal of nanomedicine, 5: 299-313.

[6] I. B. Leonor, et al. (2003) In vitro bioactivity of starch thermoplastic/hydroxyapatite composite biomaterials: an in situ study using atomic force microscopy. Biomaterials 24: 579-585.

[7] J. Ni and M. Wang (2002) In vitro evaluation of hydroxyapatite reinforced polyhydroxybutyrate composite. Materials Science and Engineering: C 20: 101-109.

[8] D. R. Ciocca, et al. (2007) A pilot study with a therapeutic vaccine based on hydroxyapatite ceramic particles and self-antigens in cancer patients. Cell stress & chaperones 12:33-43.

[9] S. Sotome, et al.(2004) Synthesis and in vivo evaluation of a novel hydroxyapatite/collagen-alginate as a bone filler and a drug delivery carrier of bone morphogenetic protein. Materials Science and Engineering: C 24: 341-347.

[10] S. Wang, et al. (2010) Towards sustained delivery of small molecular drugs using hydroxyapatite microspheres as the vehicle. Advanced Powder Technology 21:268-272.

[11] T. J. Webster, et al. (2004) Osteoblast response to hydroxyapatite doped with divalent and trivalent cations. Biomaterials 25: 2111-2122.

[12] J. Wang and L. L. Shaw (2009) Nanocrystalline hydroxyapatite with simultaneous enhancements in hardness and toughness. Biomaterials 30:6565-6572.

[13] I. Sopyan and A. Natasha (2009) Preparation of nanostructured manganese-doped biphasic calcium phosphate powders via sol–gel method. Ionics 15:735-741.

[14] C. Y. Tang, et al.(2009) Influence of microstructure and phase composition on the nanoindentation characterization of bioceramic materials based on hydroxyapatite. Ceramics International 35:2171-2178.

[15] G. K. Lim, et al.(1999) Nanosized hydroxyapatite powders from microemulsions and emulsions stabilized by a biodegradable surfactant. Journal of Materials Chemistry 9:1635-1639.

[16] Ramesh Singh, Iis Sopyan, Mohammed Hamdi (2008) Synthesis of Nano sized hydroxyapatite powder using sol-gel technique and its conversion to dense and porous body. Indian Journal of Chemistry 47:1626-1631.

[17] K. Ioku, et al.(2006) Hydrothermal preparation of tailored hydroxyapatite. Journal of Materials Science 41:1341-1344.

[18] B. Nasiri-Tabrizi, et al.(2009) Synthesis of nanosize single-crystal hydroxyapatite via mechanochemical method. Materials Letters 63:543-546.

[19] J. Salas, et al.(2009) Effect of Ca/P ratio and milling material on the mechanochemical preparation of hydroxyapaptite. Journal of Materials Science: Materials in Medicine 20:2249-2257.

[20] K. C. B. Yeong, et al.(2001) Mechanochemical synthesis of nanocrystalline hydroxyapatite from CaO and CaHPO4. Biomaterials 22:2705-2712.

[21] N. Y. Mostafa (2005) Characterization, thermal stability and sintering of hydroxyapatite powders prepared by different routes. Materials Chemistry and Physics 94:333-341.

[22] S.-H. Rhee (2002) Synthesis of hydroxyapatite via mechanochemical treatment. Biomaterials 23:1147-1152.

[23] C. C. Silva, et al.(2003) Structural properties of hydroxyapatite obtained by mechanosynthesis. Solid State Sciences 5:553-558.

[24] F. B. O. Markovic M. & Tung M S. (2004) J Res Natl Inst Stand Technol.109:553.

[25] T. Tian, et al. (2008) Synthesis of Si-substituted hydroxyapatite by a wet mechanochemical method. Materials Science and Engineering: C. 28:57-63.

[26] [F. BO. (1974) Infrared studies of apatites II. Preparation of normal and isotopically substituted calcium, strontium, and barium hydroxyapatites and spectra-structure-composition correlations. Inorganic Chemistry 13:207–214.

[27] D. Choi and P. N. Kumta (2007) Mechano-chemical synthesis and characterization of nanostructured [beta]-TCP powder. Materials Science and Engineering: C. 27: 377-381.

[28] A. G. P. C.C.Silva et al. (2004) Properties and in vivo investigation of nanocrystalline hydroxyapatite obtained by mechanical alloying. Materials Science and Engineering: C . 24: 549-554.

Corresponding Author:

Author: Dr. Iis Sopyan

Institute: Department of Manufacturing and Materials Engineering
International Islamic University Malaysia
Street: PO Box 10
City: Kuala Lumpur
Country: Malaysia
Email: sopyan@iium.edu.my